Simultaneously Strong and Tough Ultrafine Continuous Nanofibers

Dimitry Papkov,[†] Yan Zou,[†] Mohammad Nahid Andalib,[†] Alexander Goponenko,[†] Stephen Z. D. Cheng,[‡] and Yuris A. Dzenis[†,*]

[†]Department of Mechanical and Materials Engineering, Nebraska Center for Materials and Nanoscience, University of Nebraska—Lincoln, Lincoln, Nebraska 68588-0526, United States and [‡]College of Polymer Science and Polymer Engineering, University of Akron, Akron, Ohio 44325-3909, United States

ABSTRACT Strength of structural materials and fibers is usually increased at the expense of strain at failure and toughness. Recent experimental studies have demonstrated improvements in modulus and strength of electrospun polymer nanofibers with reduction of their diameter. Nanofiber toughness has not been analyzed; however, from the classical materials property trade-off, one can expect it to decrease. Here, on the basis of a comprehensive analysis of long (5−10 mm) individual polyacrylonitrile nanofibers, we show that nanofiber toughness also dramatically improves. Reduction of fiber diameter from 2.8 μm to ∼100 nm resulted in simultaneous increases in elastic modulus from 0.36 to 48 GPa, true strength from 15 to 1750 MPa, and toughness from 0.25 to 605 MPa with the largest increases recorded for the ultrafine nanofibers smaller than 250 nm. The observed size effects showed no sign of saturation. Structural investigations and comparisons with mechanical behavior of annealed nanofibers allowed us to attribute ultrahigh ductility (average failure strain stayed over 50%) and toughness to low nanofiber crystallinity resulting from rapid solidification of ultrafine electrospun jets. Demonstrated superior mechanical performance coupled with the unique macro-nano nature of continuous nanofibers makes them readily available for macroscopic materials and composites that can be used in safety-critical applications. The proposed mechanism of simultaneously high strength, modulus, and toughness challenges the prevailing 50 year old paradigm of high-performance polymer fiber development calling for high polymer crystallinity and may have broad implications in fiber science and technology.

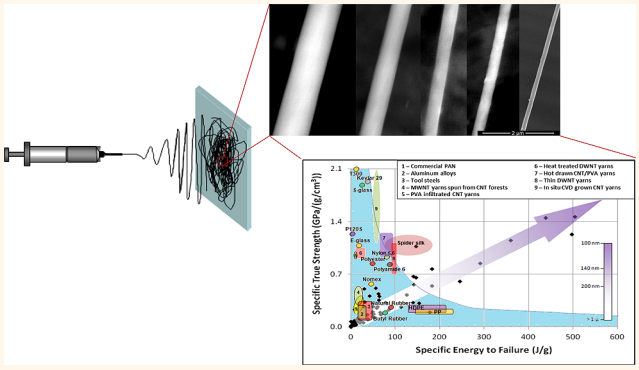

KEYWORDS: continuous nanofibers · electrospinning · size effects · strength · toughness · crystallinity

Simultaneous improvement of strength and toughness is the Holy Grail of structural materials research. Unfortunately, strength is usually improved at the expense of toughness.[1] For example, metals and polymers that are drawn to high draw ratios exhibit remarkable strength and moduli but low failure strains. Development of advanced fibers in the second half of the 20th century revolutionized structural materials. High-performance fibers, the strongest materials commercially available today, are now widely used in structural applications and composites. However, all existing advanced fibers are brittle. Even polymer fibers do not exceed 3.8% deformation at failure, while most structural fibers break at lower strains.[2]

It is well-known that the strength of fibers increases with the decrease of their diameter. Examples are well-documented and include whiskers, polymer, carbon, glass, and ceramic fibers. The mechanisms vary but are usually thought to include improvements in material structure and orientation as well as reduction in the size and quantity of defects. As a result, advanced fiber manufacturers usually adopt the smallest fiber diameter that is technologically and economically feasible. A significant industrial developmental effort in the last decades reduced carbon fiber diameter from 6.5−7 to 4.5−5 μm, leading to remarkable improvements in strength. There is a continuing interest in further diameter reduction; however, conventional mechanical spinning techniques are generally not able to produce filaments smaller than about 2 μm.

Electrospinning produces continuous nanofilaments with diameters in the range from

* Address correspondence to ydzenis@unl.edu.

Received for review January 3, 2013 and accepted March 6, 2013.

Published online March 06, 2013
10.1021/nn400028p

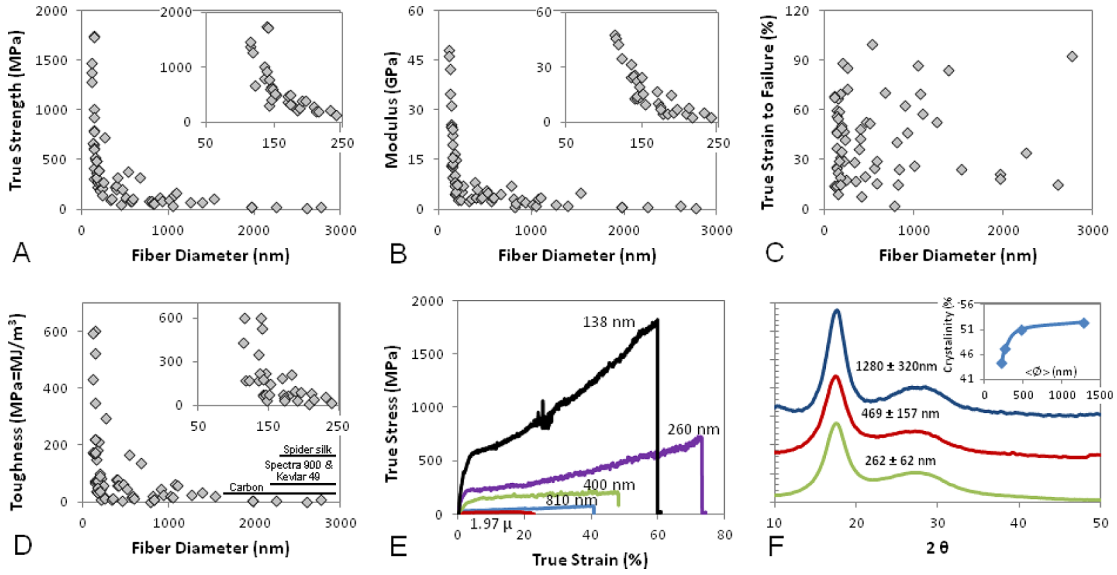

Figure 1. Size effects in mechanical properties and structure of as-spun PAN nanofibers. (A) True strength; (B) modulus; (C) true strain to failure; (D) toughness (lines indicate comparison values for several high-performance fibers and spider silk); (E) typical stress/strain behavior; (F) XRD patterns for nanofiber bundles with different average fiber diameters and variation of degree of crystallinity with average fiber diameter (inset).

single nanometers to micrometers by jetting polymer solutions in high electric fields.[3] These nanofibers exhibited some interesting mechanical properties[4] but are generally considered weak compared to conventional polymer fibers.[5] Recently, several groups, including ours, reported increases in modulus and strength with the reduction of nanofiber diameter[6−14] (see summary Table S1 in Supporting Information). However, no analysis of size effect on toughness has been yet conducted. On the basis of the classical behavior of structural materials and fibers, one would expect nanofiber strain at failure and toughness to decrease as strength and modulus increase. Here, we performed a comprehensive systematic analysis of size effects on strength, modulus, and toughness of continuous electrospun polyacrylonitrile (PAN) nanofibers in a broad range of diameters with emphasis on ultrasmall diameters.

RESULTS AND DISCUSSION

Size Effects on Mechanical Properties of Continuous Polymer Nanofibers. Continuous polyacrylonitrile nanofibers were electrospun from 8−11% polymer solutions in dimethylformamide (DMF). Fiber diameters were controlled by varying voltage and polymer concentration. Long 5−10 mm sections of individual nanofibers (the gauge length in this study) were tested in tension under constant strain rate using a nanomechanics testing system. Nanofiber diameters were measured by FE-SEM. To avoid possible radiation damage, the diameters were measured on the sections of continuous nanofibers adjacent to the tested section. Details of nanofiber fabrication, specimen preparation, mechanical testing, and structural analysis are provided in the Methods section and Supporting Information. As-spun PAN nanofibers exhibited pronounced elasto-plastic behavior with large deformations to failure. True stress and strain were used to describe material behavior at large deformations. Nanofiber modulus, failure stress (strength), strain at failure, and toughness (area under the stress−strain curve) were extracted from individual nanofiber test results. Modulus and toughness values were computed using engineering stress−strain diagrams.

Variations of the measured strength, modulus, strain at failure, and toughness with diameter of individual as-spun PAN nanofibers are presented in Figure 1A−D. Typical stress−strain diagrams of nanofibers with different diameters are shown in Figure 1E. The results (Figure 1A,B) show extraordinary increases in strength and modulus as nanofiber diameter decreases. The most dramatic increases were recorded for nanofibers finer than 200−250 nm (see insets; note that prior studies[6−14] did not cover this ultrafine range; properties of nanofibers with diameters larger than the above threshold correspond well to the previously published data[13]). The highest strength and modulus values measured in this study were 5−10 times higher than the strengths and moduli of commercial PAN fibers[5] and are on par with the highest reported strength and modulus achieved in a superdrawn (80×) ultra-high molecular weight (UHMW) PAN microfiber.[15] As mentioned above, such high values of modulus and strength in polymers are usually achieved at the expense of strain at failure. Remarkably, the high strength of the ultrafine PAN nanofibers was achieved without statistically noticeable reduction of their failure strain (Figure 1C). Though the scatter is high

(usual in fiber studies), the average strain at failure appears to slightly increase with the diameter decrease and stays well above 50%. These unique simultaneous increases in modulus, strength, and strain at failure led to a dramatic increase of toughness (Figure 1D). The highest recorded toughness was an order of magnitude higher than toughness of the best existing advanced fibers (see lines in Figure 1D) and exceeded toughness of spider silk. We observed similar behavior on several other nanofiber systems, including synthetic and biological polymers. Mechanisms of this unusual behavior need to be better understood in order to be exploited.

Possible Mechanisms of Dramatic Simultaneous Improvements in Strength, Modulus, and Toughness. Observed increases in elastic modulus and strength can be attributed to improved chain orientation in the ultrafine nanofibers. There is now extensive evidence of macromolecular orientation in electrospun fibers (see, *e.g.*, refs 7−10 and 16−18). Note that most of these studies were conducted on bundles of nanofibers of relatively large diameters (several hundreds of nanometers). Because chain orientation will only increase with the decrease of nanofiber diameters, the finest nanofibers in this study were highly oriented, which is reflected in the high values of their elastic moduli (Figure 1B). In addition to orientation, ultrahigh strength and modulus of conventional high-performance polymer fibers are usually achieved as a result of high crystallinity. The two strongest commercial polymer fibers, polyaramid (Kevlar) and UHMW polyethylene (Spectra or Dyneema), rely on specialized, crystallinity-promoting fiber spinning techniques, that is, spinning from a liquid crystalline (LC) solution and gel drawing, which result in high respective crystallinities of 75 and 95%. Most other high-performance polymer fibers, including experimental fibers under development,[2] also rely on spinning from LC solutions of rigid-rod polymers that results in high crystallinity. However, while helping to further increase strength and modulus, high crystallinity also reduces macromolecular mobility in the crystalline phase and leads to low deformations to failure. Mutual sliding mobility of long chains in the amorphous regions of semicrystalline polymers is needed for ductile, plastic behavior. Due to high crystallinity, all existing high-performance polymer fibers have very low deformations at failure compared to bulk polymers.

We have analyzed crystallinity of the as-spun PAN nanofibers by wide-angle X-ray diffraction (XRD) analysis. XRD diffractograms of nanofiber bundles with several different average nanofiber diameters are shown in Figure 1F. All XRD spectra exhibited a broad amorphous halo in addition to the crystalline peak and closely resembled the spectra of unoriented semicrystalline PAN powder and undrawn cast PAN film reported in ref 19. Degree of crystallinity (see inset in Figure 1F and Supporting Information for details of analysis) was relatively low and further decreased for the finer fiber diameters. The results are consistent with low crystallinity in as-spun PAN nanofibers observed by others.[13,20] Note that XRD measurements in the current study were performed on nanofibers with relatively broad diameter distributions (see Figure 1F). Our analysis showed significant reduction of the average crystallinity in as-spun nanofibers with reduced average nanofiber diameter. Crystallinity of the smallest nanofibers tested is expected to be lower than the average value measured for the bundle because the bundle results are dominated by the largest fibers in the sample. The latter were shown to have higher crystallinity (see inset in Figure 1F).

The observed low crystallinity of the highly oriented fine nanofibers should not be accepted *a priori* and requires an explanation. In conventional polymer fibers and films, increased macromolecular orientation achieved by drawing results in increased crystallinity.[21] It is easier for the oriented polymer chains to organize into a crystal as opposed to unoriented entangled chains. High crystallinity of the oriented PAN was demonstrated in ref 19. Drawing of PAN film in that work was shown to cause a complete disappearance of the amorphous halo in the XRD diffraction pattern, which was interpreted as a transformation of PAN from a two-phase semicrystalline polymer into a single-phase material. Analysis of PAN nanofiber crystalline structure in this study showed, however, that as-spun nanofiber crystallinity did not increase with the reduction of diameter but rather decreased for finer diameters, despite the higher chain orientation in the ultrafine nanofibers that is supported, among other things, by their high modulus. Low crystallinity in electrospun nanofibers may be the result of fast solvent evaporation from electrospun jets leading to rapid jet solidification. Indeed, solvent evaporation in electrospinning occurs rapidly in-flight, resulting in solid nanofibers deposited on a collector. Fast evaporation and solidification may preclude polymer crystallization, despite the beneficial effect of chain orientation in nanofibers. Note that smaller jets lose solvent and solidify quicker. Recent theoretical analysis of PAN/DMF jets performed in ref 22 confirmed ultrafast (milliseconds) solvent evaporation from the submicrometer jets that supports the above mechanism. Another possible mechanism of reduced crystallinity in fine nanofibers may be the high fraction of polymer located near the fiber surface. Effects of confinement on glass transition temperature[23] and elastic properties[24] were reported to extend for up to several hundred nanometers in thin polymer films. These effects might be even more pronounced in our case because of the two-dimensional nature of confinement in nanofibers. On the basis of this analysis, we conclude that crystallization in fine electrospun PAN

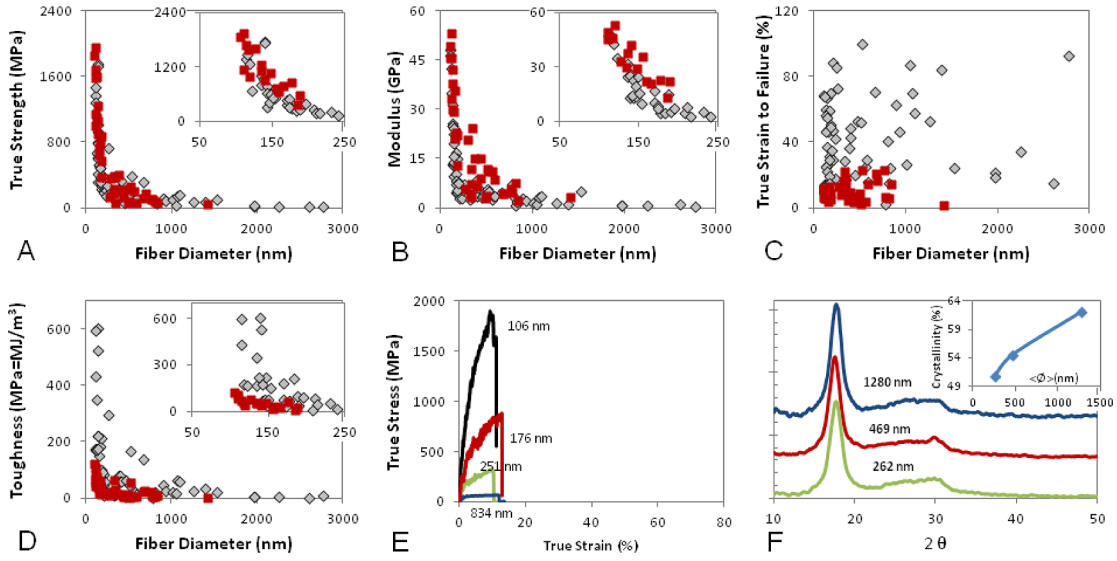

Figure 2. Comparison of size effects in as-spun and annealed PAN nanofibers. (A) True strength; (B) modulus; (C) true strain to failure; (D) toughness. In all figures, gray diamonds are for as-spun fibers and red squares for annealed fibers. (E) Typical stress/strain diagrams for annealed fibers on the same strain scale as in Figure 1E; (F) XRD spectra for annealed nanofiber bundles with different average fiber diameters. The annealed bundles were the same bundles studied in Figure 1E. Nanofiber diameter distributions were not significantly changed by the annealing. The inset shows the dependence of crystallinity on average fiber diameter for annealed nanofibers.

nanofibers is suppressed by fast solvent evaporation and rapid polymer solidification and, possibly, by two-dimensional surface confinement effects. We further hypothesize that reduced crystallinity in the ultrafine electrospun nanofibers is responsible for preserving high nanofiber ductility, while increased chain molecular orientation caused by intense jet stretching in electrospinning is responsible for high strength and modulus.

Verification of Structural Hypothesis by Analysis of Annealed Nanofibers. Direct observation of fine as-spun PAN nanofibers in low-voltage TEM and electron diffraction analysis confirmed low polymer crystallinity. However, diffuse diffraction patterns did not allow quantitative structural characterization of individual nanofibers. To further elucidate the role of crystallinity on mechanical behavior, we performed mechanical analysis of annealed nanofibers. Annealing is often used to increase the degree of crystallinity in rapidly solidified thermodynamically metastable polymers. Annealing temperature for PAN nanofibers (130 °C) was selected in the range of temperatures between PAN glass transition (90−120 °C) and oxidation temperature. Vaisman *et al.*[20] reported a sharp increase in the crystal size growth rate above 100 °C for PAN nanofibers made from polymers with a molecular weight similar to the one in our study. Oxidation of PAN, a process essential in the conversion of PAN precursors to carbon, does not usually start at temperatures below 200 °C.[25] Results of mechanical and structural evaluation of annealed PAN nanofibers are shown in Figure 2.

Wide-angle X-ray analysis confirmed the increase in crystallinity as compared to as-spun nanofibers across the range of nanofiber diameters (Figure 2F). Interestingly, similar to as-spun nanofibers, the degree of crystallinity of annealed samples also decreased with the decrease of average nanofiber diameter. This may be due to the differences in the initial structure of the nanofibers (see data for as-spun nanofibers of different diameters in Figure 1F). Variations of mechanical properties of individual annealed PAN nanofibers are compared with as-spun PAN nanofiber properties in Figure 2A−D. Typical stress−strain diagrams of annealed nanofibers are plotted in Figure 2E in the same strain scale as as-spun nanofiber diagrams in Figure 1E for easier comparison. The analysis shows a significant increase in modulus compared to as-spun nanofibers of similar diameters. Strength values were also higher. However, nanofiber failure strain sharply decreased. The measured strains at failure of annealed nanofibers shown in Figure 2C are within the range of strains typical of commercial textile polymer fibers such as polyester, polyamide 6, nylon 66, and Nomex.[26] Textile fibers have higher strains to failure than advanced high-performance fibers, such as Kevlar and Spectra/Dyneema, but exhibit lower strength and modulus. Annealed PAN nanofibers still exhibited a strong size effect in modulus and strength. However, significantly, the observed sharp reduction of strain at failure led to reduction of toughness (Figure 2D). Overall, these results correlate with the increased crystallinity of the annealed nanofibers and support our hypothesis that large strains at failure and ultrahigh toughness of as-spun nanofibers are due to their low crystallinity.

Analysis of Strength−Toughness Correlation and Comparison to Conventional and Developmental Materials. To further

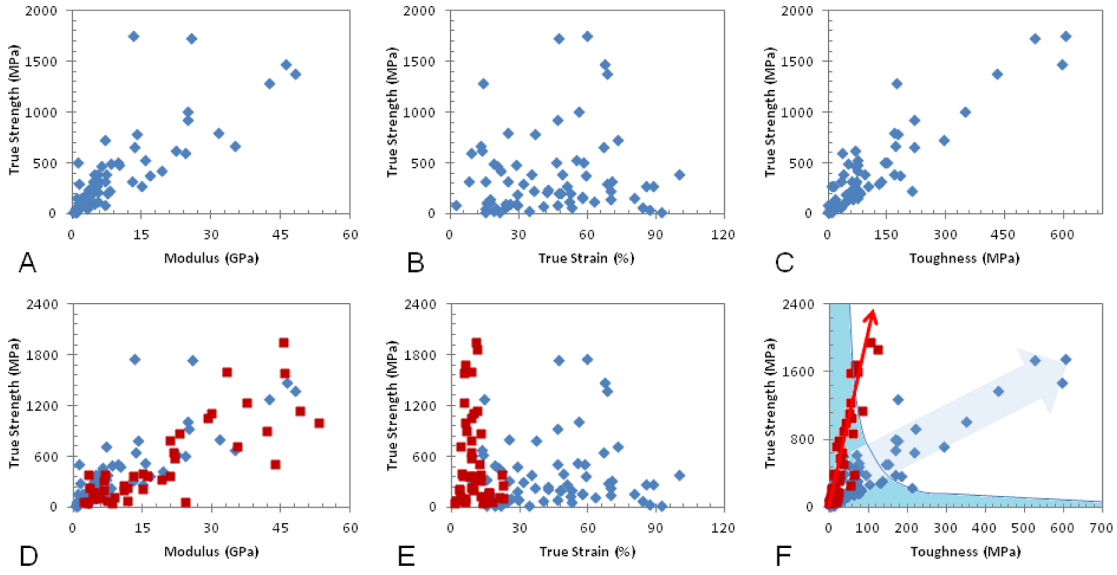

Figure 3. Correlations of mechanical properties of nanofibers of different diameters. (A–C) As-spun fibers: (A) true strength *vs* modulus; (B) true strength *vs* true strain to failure; (C) true strength *vs* toughness. (D–F) Comparison between as-spun (blue diamonds) and annealed (red squares) nanofibers: (D) true strength *vs* modulus; (E) true strength *vs* true strain to failure; (F) true strength *vs* toughness. Arrows in (F) point in the directions of decreasing nanofiber diameters.

analyze the size effects in electrospun nanofibers, we plotted and studied correlations between various mechanical characteristics (Figure 3; see details of statistical analysis in Supporting Information). A relatively good correlation (within typical high scatter in fiber studies) was observed for strength and modulus in both as-spun and annealed nanofibers (Figure 3A,D; computed coefficients of determination $r^2 = 0.65$ and 0.76, respectively). The strength–modulus correlation is generally expected and is often observed in structural materials and fibers as a result of processes aimed at material strengthening. Interestingly, the data for the as-spun and annealed nanofibers overlap, as seen in Figure 3D, indicating that relative stiffening of the annealed nanofibers occurred simultaneously with their strengthening. The observed correlation supports macromolecular chain orientation as the mechanism responsible for improvements in both modulus and strength. The strength–failure strain plots (Figure 3B,E) did not show any correlation (the slope of the regression curve was not statistically different from zero at $\alpha = 0.05$ confidence level), and the strain at failure was randomly distributed across the strength range for both nanofiber systems. However, strong correlation was observed for strength and toughness (Figure 3C,F; $r^2 = 0.82$ and 0.77 for the as-spun and annealed nanofibers, respectively; the arrows in Figure 3F point in the direction of decreasing nanofiber diameters). The observed strong strength–toughness correlation is unusual in structural materials. Although some biological composite materials, such as spider silk, through their hierarchical structure, attain simultaneously high strength and toughness, most engineering materials exhibit strength–toughness trade-off, revealing that high strength is usually achieved at low toughness and *vice versa* (see shaded area in Figure 3F). Most processing techniques improving the strength of the originally ductile materials, such as metals or semicrystalline polymers, cause the material parameters to move from the bottom right to the top left corner of the strength–toughness diagram. This applies to such widely used processes as drawing of polymers and metals and to newer processes, such as nanostructuring of metals.[27] High-performance fibers also follow this trend, all exhibiting high tensile strength but relatively low toughness. Reaching the upper right corner of the diagram in Figure 3F is highly desirable for safety-critical applications requiring both high strength and fracture resistance.[1] Demonstrated consistent shift of the properties of as-spun electrospun nanofibers toward the upper right corner with the reduction of diameter is encouraging. While annealed nanofibers exhibited lower toughness compared to as-spun PAN nanofibers, their strain at failure still did not appear to decrease with the decrease of diameter (and corresponding increase in strength), resulting in steeper but still positive correlation between strength and toughness (Figure 3F). Moreover, multiple regression analysis (see Supporting Information) shows that the slope of the strength–toughness correlation for the annealed nanofibers is decreasing for higher strength values, indicating a larger toughness increase. This suggests that change of crystallinity *via* annealing or other methods can be used to alter nanofiber properties and provides the means to expand the coverage of the strength–toughness performance space. Note that the highest toughness of annealed nanofibers was still in the range

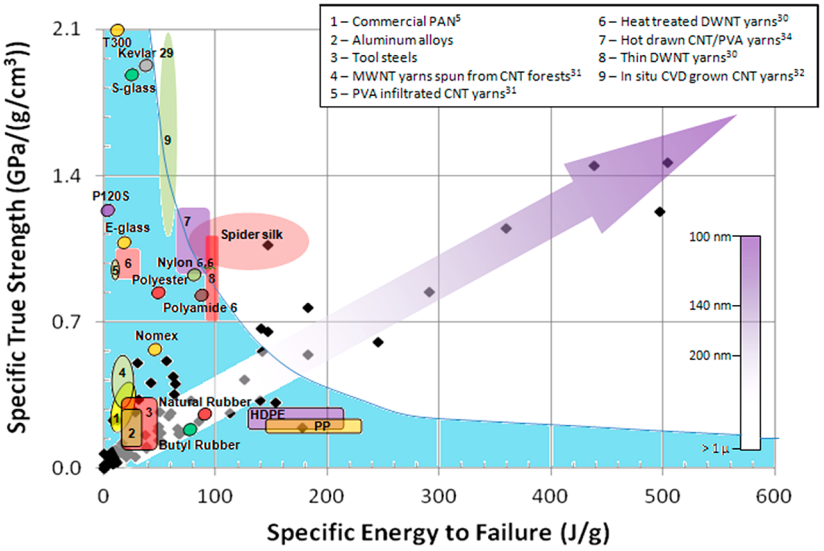

Figure 4. Comparison of specific strength and specific energy to failure of as-spun PAN nanofibers (diamonds) with typical values for commercial and developmental fibers and materials.[2,5,26,30−32,34] The arrow density indicates approximate values of nanofiber diameters (see scale bar). The colored area represents the strength/toughness region occupied by traditional materials.

of the toughness values of spider silk. Compared to spider silk, the best annealed nanofibers had lower strain at failure but higher strength—a property combination that may be useful for ballistic applications.

The magnitudes of the mechanical improvements in the current study are among the strongest size effects recorded for any material. While most fibrous materials exhibit increases in strength with diameter decrease (observation of diameter dependence of strength in glass fibers triggered the development of modern fracture mechanics theory[28]), these increases usually are moderate. Reduction of as-spun PAN nanofiber diameter from 2.8 μm to ~100 nm resulted in simultaneous increases in modulus from 0.36 to 48 GPa, true strength from 15 to 1750 MPa, and toughness from 0.25 to 605 MPa. The relative increases in modulus and strength far exceed the size effects reported for the electrospun nanofibers in refs 6−13. Size effects on toughness have not been previously reported.

Figure 4 compares specific strength and toughness of as-spun PAN nanofibers with properties of some commercial and developmental fibers and structural materials. The arrow color density indicates approximate nanofiber diameter values (see the scale bar). It can be seen that the properties of most existing structural materials and fibers are within the shaded area of the diagram, demonstrating classical strength−toughness trade-off. Spider silk is one natural material providing exceptionally high toughness at high strength. In addition, several recent carbon nanotube (CNT)-based fibers and yarns showed promising combinations of specific strength and energy-to-failure. Analysis of Figure 4 shows that fine continuous nanofibers in this study outperformed most existing and developmental CNT-based fibers in terms of toughness. The best recorded properties of nanofibers far exceeded the properties of conventional PAN microfibers (250−400 MPa strength and 3−8 GPa modulus[5]) and exceeded the strength of all commercial polymer textile fibers (such as polyester, Nomex, polyamide 6, and nylon 66[26]) while exhibiting 6−10-fold higher toughness. The best recorded strengths of as-spun PAN nanofibers were on par with the high-strength spider silk[29] while showing three times higher toughness (spider silk is regarded as the toughest strong material known). Finally, best as-spun PAN nanofibers outperformed most developmental CNT fibers,[30−32] while approaching the level of performance of the toughest CNT fibers reported to date.[33,34] Encouragingly, all trends analyzed in this study do not show signs of saturation, indicating a strong possibility of further performance improvements.

It is interesting to note that the diameter range exhibiting most significant mechanical improvements in this study (<250 nm) overlaps with the range of diameters of biological fibers, such as collagen fibrils.[35] Polymer fibers are ubiquitous in biological materials and tissues and are commonly thought to be responsible for their superior mechanical properties and toughness. Silk fibers have been shown to possess nanofibrillar structure with nanofibrills ranging from 25 to 170 nm.[36,37] Further studies of molecular mechanisms of mechanical behavior of continuous nanofibers may shed light on the nature of strength and toughness in biological materials, which could lead to novel biomimetic structural materials with unusual properties.[1]

SUMMARY AND CONCLUSIONS

In summary, ultrafine as-spun PAN nanofibers exhibited extraordinary simultaneous strength, modulus,

and toughness. Structural analysis and experiments on annealed nanofibers suggest that low crystallinity in electrospun nanofibers is responsible for the exceptionally high nanofiber ductility and toughness. We note that the observed decrease in polymer crystallinity with electrospun nanofiber diameter may not be universal. Polymer crystallization is a complex process that depends on a large number of parameters and processing conditions, and the atactic polyacrylonitrile may be prone to produce lower crystallinity. Supporting Information Table S1 points to some examples showing increased nanofiber crystallinity with diameter decrease. Incidentally, these studies also exhibited low or decreasing strains to failure. However, other studies[3,38] and our own preliminary analysis of several other nanofiber families indicate that other polymer systems may exhibit behaviors similar to the one described in this study. Peculiarities of crystallization during complex coupled electrospinning process (this technique combines electrical, mechanical, mass transfer, and thermal phenomena in a single multiphysics process) are yet to be studied and control may not be easy. Models of polymer jets incorporating solvent evaporation and polymer solidification can provide insights.[22] Continuous nanofibers with simultaneously high strength, modulus, and toughness can be used in a broad variety of structural materials and composites.[38] Their unique dual nano-macro nature provides an easy way to bridge scales and makes them readily available for macroscopic applications. Our proposed structural explanation of the observed superior combination of nanofiber mechanical properties challenges the prevailing paradigm of high-performance polymer fiber development, that is, achieving high crystallinity with alignment, and may have broad implications for structural fibers research.

METHODS

Materials and Fiber Fabrication. PAN fibers were electrospun at ambient conditions from 8−11 wt % solution of the polymer (Pfaltz and Bauer, Inc.; cat# P21470, MW 150 000) in DMF (Sigma-Aldrich; cat# 271012) using a 20 gauge needle. Fibers were collected on a stationary target. The applied voltage was 10−12 kV; the distance between the spinneret and collector was 20 cm. Fiber diameters were varied by varying the voltage and PAN concentration. As-spun and annealed fibers were prepared using similar electrospinning parameters. Annealing was performed at 130 °C in air for 1 h.

Specimen Preparation and Mechanical Testing. Individual fibers were mechanically tested in a NANO UTM testing system (MTS) under a constant strain rate of 0.001 s^{-1}. Fibers of 4−5 cm in length were electrospun on a split electrode. Individual fibers were picked up with a wire "fork". A 5−10 mm section of the fiber (the gauge length in this study) was transferred and glued to the grips of the testing machine with an epoxy adhesive. An adjacent section of the same fiber was examined using a Quanta 200 FEG SEM (FEI). Its diameter was measured in at least three places and averaged for the purpose of calculating the mechanical properties. As-spun fibers exhibited elasto-plastic behavior with large deformations to failure. Measured load and displacement variations were converted to engineering and true stresses and strains and plotted as stress−strain diagrams. True stress and strain are often used to describe material behavior at large deformations. Nanofiber modulus, failure stress (strength), strain at failure, and toughness (area under the curve) were calculated from the obtained stress−strain diagrams. Modulus and toughness were computed using engineering stress−strain diagrams. The total numbers of tests were 65 for the as-spun nanofibers and 43 for the nanofibers annealed at 130 °C.

X-ray Structural Analysis. Nanofiber mats were electrospun for structural analysis onto an aluminum substrate. Average fiber diameter and standard deviation were measured using SEM (at least 200 fibers from several locations were evaluated for each sample). Wide-angle X-ray diffraction (XRD) analysis was performed using a Rigaku Multiflex X-ray diffractometer with Cu Kα radiation in the range of 2θ between 10 and 50°. The background was removed, and the crystalline peak (or peaks in the case of annealed samples) and the amorphous halo were fitted using Lorentzian peak shapes, as illustrated in Figure S1 in Supporting Information. At least three samples with different average nanofiber diameters were analyzed for each nanofiber family (*i.e.*, as-spun nanofibers and annealed nanofibers).

Conflict of Interest: The authors declare no competing financial interest.

Acknowledgment. This work was supported by NSF (NIRT-0709333; CMMI-0600675/0600733; CBET-1140065; DMR-0906898), AFOSR (Award No. FA9550-11-1-0204), and ARO (MURI; Award No. W911NF-09-1-0541). The authors thank Elham Forouzesh and Julia Kostogorova-Beller for initial experiments, Jeff Shield for help with the initial XRD analysis, and Ken Reifsnider, Peter Fratzl, Larry Drzal, Jack Gillespie, and Tony Bunsell for valuable discussions.

Supporting Information Available: (1) Size effects in nanofibers reported in the literature, including corresponding reports on crystallinity and polymer chain orientation; (2) explanation of the data reduction protocol for XRD experiments; (3) statistical analysis of correlations of mechanical properties of nanofibers. This material is available free of charge *via* the Internet at http://pubs.acs.org.

REFERENCES AND NOTES

1. Ritchie, R. O. The Conflicts between Strength and Toughness. *Nat. Mater.* **2011**, *10*, 817–822.
2. Committee on High-Performance Structural Fibers for Advanced Polymer Matrix Composites, National Research Council. In *High-Performance Structural Fibers for Advanced Polymer Matrix Composites*; The National Academies Press: Washington, DC, 2005.
3. Dzenis, Y. A. Spinning Continuous Fibers for Nanotechnology. *Science* **2004**, *304*, 1917–1919.
4. Naraghi, M.; Chasiotis, I.; Kahn, H.; Wen, Y.; Dzenis, Y. Mechanical Deformation and Failure of Electrospun Polyacrylonitrile Nanofibers as a Function of Strain Rate. *Appl. Phys. Lett.* **2007**, *91*, 151901–3.
5. Hou, H.; Ge, J. J.; Zeng, J.; Li, Q.; Reneker, D. H.; Greiner, A.; Cheng, S. Z. D. Electrospun Polyacrylonitrile Nanofibers Containing a High Concentration of Well-Aligned Multiwall Carbon Nanotubes. *Chem. Mater.* **2005**, *17*, 967–973.
6. Tan, E. P. S.; Lim, C. T. Physical Properties of a Single Polymeric Nanofiber. *Appl. Phys. Lett.* **2004**, *84*, 1603–1605.
7. Lim, C. T.; Tan, E. P. S.; Ng, S. Y. Effects of Crystalline Morphology on the Tensile Properties of Electrospun Polymer Nanofibers. *Appl. Phys. Lett.* **2008**, *92*, 141908−141908–3.
8. Wong, S. C.; Baji, A.; Leng, S. Effect of Fiber Diameter on Tensile Properties of Electrospun Poly(ε-caprolactone). *Polymer* **2008**, *49*, 4713–4722.

9. Arinstein, A.; Burman, M.; Gendelman, O.; Zussman, E. Effect of Supramolecular Structure on Polymer Nanofibre Elasticity. *Nat. Nanotechnol.* **2007**, *2*, 59–62.
10. Pai, C.; Boyce, M. C.; Rutledge, G. C. Mechanical Properties of Individual Electrospun PA 6(3)T Fibers and Their Variation with Fiber Diameter. *Polymer* **2011**, *52*, 2295–2301.
11. Chew, S., Y.; Hufnagel, T. C.; Lim, C., T.; Leong, K. W. Mechanical Properties of Single Electrospun Drug-Encapsulated Nanofibres. *Nanotechnology* **2006**, *17*, 3880.
12. Shin, M. K.; Kim, S. I.; Kim, S. J.; Kim, S.; Lee, H.; Spinks, G. M. Size-Dependent Elastic Modulus of Single Electroactive Polymer Nanofibers. *Appl. Phys. Lett.* **2006**, *89*, 231929-3.
13. Naraghi, M.; Arshad, S. N.; Chasiotis, I. Molecular Orientation and Mechanical Property Size Effects in Electrospun Polyacrylonitrile Nanofibers. *Polymer* **2011**, *52*, 1612–1618.
14. Papkov, D.; Zou, Y.; Dzenis, Y. Structure and Mechanical Properties of Continuous Polymer and Carbon Nanofibers. MRS Fall Technical Meeting, Boston, MA, November 28—December 2, 2011; Materials Research Society: Warrendale, PA, 2011.
15. Sawai, D.; Fujii, Y.; Kanamoto, T. Development of Oriented Morphology and Tensile Properties upon Superdawing of Solution-Spun Fibers of Ultra-High Molecular Weight Poly(acrylonitrile). *Polymer* **2006**, *47*, 4445–4453.
16. Kakade, M. V.; Givens, S.; Gardner, K.; Lee, K. H.; Chase, D. B.; Rabolt, J. F. Electric Field Induced Orientation of Polymer Chains in Macroscopically Aligned Electrospun Polymer Nanofibers. *J. Am. Chem. Soc.* **2007**, *129*, 2777–2782.
17. Kongkhlang, T.; Tashiro, K.; Kotaki, M.; Chirachanchai, S. Electrospinning as a New Technique To Control the Crystal Morphology and Molecular Orientation of Polyoxymethylene Nanofibers. *J. Am. Chem. Soc.* **2008**, *130*, 15460–15466.
18. Zong, X. H.; Kim, K.; Fang, D.; Ran, S.; Hsiao, S. H.; Chu, B. Structure and Process Relationship of Electrospun Bioabsorbable Nanofiber Membranes. *Polymer* **2002**, *43*, 4403–4412.
19. Bashir, Z.; Tipping, A. R.; Church, S. P. Orientation Studies in Polyacrylonitrile Films Uniaxially Drawn in the Solid State. *Polym. Int.* **1994**, *33*, 9–17.
20. Vaisman, L.; Wachtel, E.; Wagner, H. D.; Marom, G. Polymer—Nanoinclusion Interactions in Carbon Nanotube Based Polyacrylonitrile Extruded and Electrospun Fibers. *Polymer* **2007**, *48*, 6843–6854.
21. Ziabicki, A.; Kawai, H. *High-Speed Fiber Spinning: Science and Engineering Aspects*; Wiley: New York, 1985; p 586.
22. Wu, X.; Salkovskiy, Y.; Dzenis, Y. A. Modeling of Solvent Evaporation from Polymer Jets in Electrospinning. *Appl. Phys. Lett.* **2011**, *98*, 223108.
23. Priestley, R. D.; Ellison, C. J.; Broadbelt, L. J.; Torkelson, J. M. Structural Relaxation of Polymer Glasses at Surfaces, Interfaces, and In Between. *Science* **2005**, *309*, 456–459.
24. Watcharotone, S.; Wood, C. D.; Friedrich, R.; Chen, X.; Qiao, R.; Putz, K.; Brinson, L. C. Interfacial and Substrate Effects on Local Elastic Properties of Polymers Using Coupled Experiments and Modeling of Nanoindentation. *Adv. Eng. Mater.* **2011**, *13*, 400–404.
25. Vaisman, L.; Larin, B.; Davidi, I.; Wachtel, E.; Marom, G.; Wagner, H. D. Processing and Characterization of Extruded Drawn MWNT-PAN Composite Filaments. *Composites, Part A* **2007**, *38*, 1354–1362.
26. Bunsell, A., R. Fibre Reinforcements for Composite Materials. In *Composite Materials*; Pipes, R. B., Ed.; Elsevier: New York, 1988; Vol. 2, p 537.
27. Zhu, Y. T.; Liao, X. Nanostructured Metals: Retaining Ductility. *Nat. Mater.* **2004**, *3*, 351–352.
28. Griffith, A. A. The Phenomena of Rupture and Flow in Solids. *Philos. Trans. R. Soc., A* **1921**, *221*, 163–198.
29. Vollrath, F.; Knight, D. P. Liquid Crystalline Spinning of Spider Silk. *Nature* **2001**, *410*, 541–548.
30. Naraghi, M.; Filleter, T.; Moravsky, A.; Locascio, M.; Loutfy, R. O.; Espinosa, H. D. A Multiscale Study of High Performance Double-Walled Nanotube—Polymer Fibers. *ACS Nano* **2010**, *4*, 6463–6476.
31. Zhang, M.; Atkinson, K. R.; Baughman, R. H. Multifunctional Carbon Nanotube Yarns by Downsizing an Ancient Technology. *Science* **2004**, *306*, 1358–1361.
32. Motta, M.; Moisala, A.; Kinloch, I. A.; Windle, A. H. High Performance Fibres from `Dog Bone' Carbon Nanotubes. *Adv. Mater.* **2007**, *19*, 3721–3726.
33. Dalton, A. B.; Collins, S.; Munoz, E.; Razal, J. M.; Ebron, V. H.; Ferraris, J. P.; Coleman, J. N.; Kim, B. G.; Baughman, R. H. Super-Tough Carbon-Nanotube Fibres. *Nature* **2003**, *423*, 703–703.
34. Miaudet, P.; Badaire, S.; Maugey, M.; Derre, A.; Pichot, V.; Launois, P.; Poulin, P.; Zakri, C. Hot-Drawing of Single and Multiwall Carbon Nanotube Fibers for High Toughness and Alignment. *Nano Lett.* **2005**, *5*, 2212–2215.
35. Fratzl, P. Cellulose and Collagen: From Fibres to Tissues. *Curr. Opin. Colloid Interface Sci.* **2003**, *8*, 32–39.
36. Putthanarat, S.; Stribeck, N.; Fossey, S. A.; Eby, R. K.; Adams, W. W. Investigation of the Nanofibrils of Silk Fibers. *Polymer* **2000**, *41*, 7735–7747.
37. Zhao, H.; Feng, X.; Gao, H. Ultrasonic Technique for Extracting Nanofibers from Nature Materials. *Appl. Phys. Lett.* **2007**, *90*, 073112-073112-2.
38. Dzenis, Y. A. Structural Nanocomposites. *Science* **2008**, *319*, 419–420.